Polymer Testing 146 (2025) 108747

Contents lists available at ScienceDirect

Polymer Testing

journal homepage: www.elsevier.com/locate/polytest

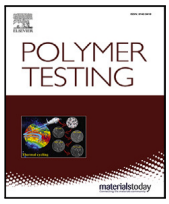

Evaluation of the time–temperature superposition by comparing neat and glass-fibre-reinforced epoxy using dynamic mechanical thermal analysis

Daniel Esse [a,*], Benedikt Scheuring [a], Frank Henning [b], Wilfried V. Liebig [a]

[a] Karlsruhe Institute of Technology, Institute for Applied Materials, Engelbert-Arnold-Straße 4, Karlsruhe, 76131, Germany
[b] Fraunhofer Institute for Chemical Technology ICT, Joseph-von-Fraunhofer-Straße 7, Pfinztal, 76327, Germany

ARTICLE INFO

Keywords:
DMA
TTS
Epoxy
Fibre-reinforced polymers
Thermorheologically simple material behaviour

ABSTRACT

Dynamic mechanical thermal analysis is a well-established method to determine the influence of temperature and frequencies on polymers. One challenge inherent to this method is the potential for significant changes in material properties, which can exceed several orders of magnitude and rapidly approach the accuracy or mechanical limits of measurement systems or actuators. In this work, it is shown that a change in the magnitude of the mechanical load within the linear elastic region does not affect the results. Consequently, the test parameters during the DMTA to be adapted to the stiffness of the specimens, allowing materials and volumes closer to the limits of the testing system to be measured. Furthermore, master curves were generated according to the temperature–time superposition for the frequency from the measured sections using a modified method. This was achieved by shifting the loss factor and applying the shift factor to the storage modulus. The tests presented in this work were carried out on continuous fibre-reinforced epoxy resin with a $[+45/-45]_{2s}$ fibre orientation and the neat matrix material itself, up to temperatures above the glass transition area. Wicket plots indicated thereby that the temperature–time superposition is applicable for both material systems. A comparison of the two material systems showed, that the fibre-reinforced specimen is shifted horizontally to a greater extent.

1. Introduction and motivation

Polymeric materials, hence also fibre-reinforced polymers, show a viscoelastic behaviour above and below the glass transition temperature T_g. In particular, the dynamic mechanical thermal analysis (DMTA) is a well established method to determine the influence of temperature and frequencies or durations on polymers and composite materials and other viscoelastic properties, including crosslinking density [1], dynamic fragility [2], dynamic or complex viscosity, storage and loss modulus, as well as creep and stress–relaxation compliance [3]. Numerical approaches have shown that the viscoelastic behaviour in the frequency domain can be calculated even for fibre-reinforced materials [4].

The mechanical properties of polymers with a viscoelastic material behaviour have both a clear time dependency and a pronounced temperature dependency. These dependencies can be explained by molecular movement and rearrangement processes, which can be thermally activated and accelerated with increasing temperature. This relationship makes it possible to use the temperature–time superposition (TTS) to convert a temperature dependence into a time dependency [5]. To cover a wide range of material properties, this superposition is established, allowing predictions of material behaviour at temperatures or loading rates that cannot be measured in the laboratory or are impractical to measure. Here, the effect of a long-term load at a constant load rate and temperature can be converted to the effect of a load at a higher temperature or shorter time and vice versa [6].

In general, when TTS is used, materials can be classified as thermorheologically simple or complex. For materials that are thermorheologically simple, a change in temperature is equivalent to a change in the behaviour of the material only along the logarithmic frequency or time axis. This shift can be interpreted as evidence that the temperature changes effectively accelerate or retard the dominant viscoelastic processes [7]. This allows the creation of a master curve by shifting the properties of the measured material to different frequencies or durations [8]. The individual curves of a multiplex versus the logarithmic frequency are shifted horizontally along the frequency axis until they overlap with the neighbouring curve. The shift factor a_T is therefore a function of temperature and is given by Eq. (1) [9].

$$a_T = \frac{f_0}{f_T} = \frac{t_T}{t_0}. \tag{1}$$

* Corresponding author.
E-mail address: daniel.esse@kit.edu (D. Esse).

https://doi.org/10.1016/j.polymertesting.2025.108747
Received 19 November 2024; Received in revised form 19 February 2025; Accepted 25 February 2025
Available online 18 March 2025

The frequency at which the material achieves a particular response at temperature T is represented by f_T, while f_0 represents the frequency at which the material achieves the same response at the reference temperature T_0. To predict the ageing or long-term properties of a material, one can use the fact that frequency is inversely proportional to time [6]. The time t in Eq. (1) is indexed similarly to the frequency. To extend the range of frequency studies to very low or high frequencies outside the scanning range of the DMTA instrument, data are often added from creep or free resonance experiments. Data from these tests can only be added if the material behaves similarly in these experiments to a dynamic scan [6].

Materials in which the type and number of molecular movement and rearrangement processes change with temperature are thermorheologically complex materials [10]. This means that additional vertical displacements are necessary in order to correctly shift the material behaviour outside the experimentally determined time or frequency range [11]. Particular in blends, the different components of the material will in general display a different temperature dependent rheology [12]. Furthermore, thermorheological complexity can also occur in heterogeneous solids where two or more relaxation processes are present, each with different temperature dependencies [7]. The use of TTS is not reliable if the material undergoes a phase transformation within the temperature range of interest [12] or the general chemical or physical structure chances during the measurement [13]. To check whether the assumptions of TTS hold for a material, the Cole-Cole plot [14] (log E'' versus log E'), van-Gurp-Palmen (tan(δ) versus E*) or Wicket plot (tan(δ) versus E') can be used by plotting the phase angle against the complex modulus. This eliminates the effect of the shift along the frequency and gives temperature independent curves if the TTS is valid. It also gives a direct indication of the magnitude of the resulting vertical shift [12]. A curve that looks like an arc should result from these plots [6].

Two models are commonly used to shift along the log frequency or time axis. The first is the Arrhenius equation, which is typically used for relaxations below T_g in amorphous and some crystalline polymers. The second is the Williams-Landel-Ferry equation, which describes the effect of temperature near the glass-transition temperature. Both of these methods are well documented in the literature [6–8,12] and require knowledge of specific material parameters. If these material parameters are unknown, there are several published methods to form the master curve from a multiplex. In 1993 Honerkamp and Weese introduced the nonlinear regression method, to supplement the graphical methods which were commonly used until then. They recommended approximating the individual curves by a polynomial function and calculating the shift factors by minimising the sum of the difference between the fitted curves [15]. Similar approaches were used in the publications of Kraus and Niederwald [16] and of Gergesova et al. [17]. The latter described the generalised closed-form shifting (CFS) methodology to calculate the horizontal shift of the loss factor by the evaluation of the horizontally overlapping areas between two curves [17]. While Kraus and Niederwald fitted the curves of the storage modulus to calculate the inverse function. With this intermediate step, they were able to determine the shift factor with the root-mean-square distance between two neighbouring curves [16]. The method published by Naya et al. estimates the shift factors by minimising the distance between the derivatives of the elastic modulus curves and the derivative of the curve at the reference temperature [18]. This method assumes that the horizontal shifts of the curves match with the horizontal shifts of their derivatives. A different approach, the minimisation of arc length, was used in the method published by Cho. This method assumes that, if S, the sum of the distances between adjacent data points, can be calculated by using the Pythagorean theorem, the perfect superposition gives a shorter distance than the imperfect superposition. By guessing the values of the shift factors, calculating S and repeating this, until the minimum of S is found, the master curve should be obtained [19]. An additional approach to obtaining the factors via a viscoelastic model, which provides physical significance, was published by Guedes [20]. It is known that the loss factor, as a ratio between the loss and storage moduli, does not require any vertical shift. Therefore, the shift factors obtained from the loss factor can be used for the horizontal shifting of other viscoelastic functions, which can then be adjusted vertically to account for the effect of temperature and thermal expansions [7].

One challenge that must be overcome with these two methods is the change in material properties over several orders of magnitude, which can quickly push measurement systems or actuators to their limits. On the one hand, low temperatures lead to strains that can hardly be detected by the measurement systems, or forces for which the machines are not designed. On the other hand, the low stiffness at elevated temperatures tends to invalidate the tests owing to the creeping behaviour of the material. George et al. for example, reported that they were unable, to measure the storage modulus of a photopolymer at the desired temperature of 110 °C owing to the high softening of the sheets at these temperatures. Therefore, they measured up to 90 °C and extrapolated the value of the storage modulus to 110 °C [21]. Also Schalnat et al. stated about the challenge, that owing to the very limited load range of most DMA equipment and because of the lower deformation, loading fixtures such as tensile or compression are typically not suited for determining the viscoelastic response of rigid polymer bulk [22]. Furthermore, Shao and Lee-Sullivan and Lee-Sullivan and Dykeman [23,24] state that higher amplitudes result in lower standard deviations of the results. Limitations on the amplitude are dynamic effects, the upper force of the instrument and higher strains which may fall outside the linear viscoelastic region of the specimen [22]. The smaller for example the amplitude, the more important the geometric accuracy of the specimen becomes to ensure correct load transfer from the fixture to the specimen [25]. A final validation is only possible through counter-testing at the selected temperature over the time range of the superposition curve. The validation is subject to limitations imposed by the frequency range of the testing machine or measuring device, as well as the duration of the test itself [10,26].

Throughout this study, a DMTA was performed, revealing difficulties owing to changes in material stiffness. This was encountered by a stepwise change in magnitude of the mechanical load during the DMTA. In addition, master curves according to the TTS for the frequency were generated from the determined measured sections by using a modified variant of the method published by Kraus and Niederwald, which is used to merge the multiplex of curves into one master curve [16]. Furthermore, the Wicket plots of the materials are shown, to discuss whether the TTS is applicable to the material. The tests presented in this work were carried out on continuous fibre-reinforced epoxy resin and the matrix material itself, up to temperatures above the glass transition area, which enabled a comparison between the two material systems.

2. Material and methods

2.1. Material system and manufacturing

The DMTA was carried out on continuous fibre-reinforced epoxy resin and the matrix material itself, consisting of the Resoltech 1500 resin based on diglycidyl ether of bisphenol A (DGEBA) combined with the Resoltech 1504 hardener based on 3-aminomethyl-3,5,5-trimethylcyclohexylamine. For the reinforced specimens, eight layers of unidirectional E-glass-fibre fabrics, supplied by HaLarit Composites, with 416 g/m^2 were used and manufactured with an orientation of $[+45/-45]_{2s}$ relative to the loading direction. The material was manufactured as shown in Fig. 1 by using resin transfer moulding (RTM). After placing the fibre fabrics in the 2.5 mm thick mould, the resin was injected by applying 3 bar in the pressure chamber and a vacuum of the opposite side in the vacuum chamber, to remove the air and excess resin.

Post-curing was carried out according to the manufacturer's instructions to achieve a T_g of 141 °C. Specimens 200 mm long, 25 mm wide and 2.5 mm thick were cut from the plaques by waterjet cutting. The free length of the specimens during the DMTA was 100 mm.

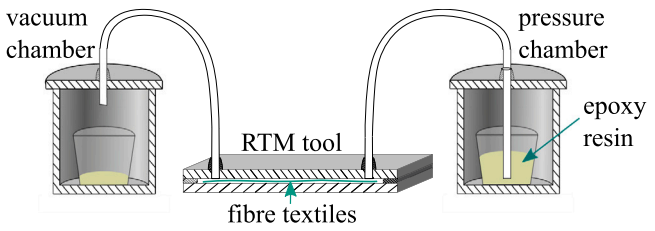

Fig. 1. Schematic setup for resin transfer moulding for the manufacturing of the specimens.

2.2. Experimental characterization

Tensile frequency sweeps were measured stress-controlled with a load ratio of 0.5 on an electropulse E3000 from Instron. To obtain the DMTA multiplex, the specimens were held at a series of isotherms with temperatures ranging from 25 °C to 180 °C, with the five logarithmically evenly distributed frequencies 0.32 Hz, 0.56 Hz, 1 Hz, 1.78 Hz and 3.2 Hz at each temperature. The load amplitudes were adjusted during the test according to the properties of the specimens, keeping the maximal displacement at approximately 0.1%. This was done with a total of five different load amplitudes, three were adjusted in 20 °C increments around T_g and one before 100 °C and one after 160 °C, where the changes in material stiffness are expected to be small. The temperature was adjusted in 5 °C steps up to 100 °C and in 2.5 °C steps at higher temperatures. During performing the test, the temperature, the amplitude of the load, the amplitude of the specimen's displacement and the phase shift between the sine waves of the displacement and the load are recorded.

2.3. Processing of the measurements

In order to evaluate the applicability of the TTS, a Wicket plot is generated for the multiplex of the isotherms. Master curves for the frequency were generated by using a modified variant of the method published by Kraus and Niederwald. The first distinction is that the curves are fitted with an exponential function, which ensures the formation of the inverse function. Secondly, the loss factor was used for horizontal shifting, in order to be able to recognise any possible need for vertical shifting. After forming the inverse functions, the incremental shift factor is calculated by the root-mean-square distance between the overlapping areas of two isotherms. If two curves did not overlap, both were extrapolated up to one decade. The incremental shift factors were then added up to form the master curve for the loss factor. Finally, the shift factors derived from the loss factor were applied to the isotherms of the storage modulus.

3. Results

The temperature sweeps for the complex tensile modulus and the loss factor are shown in Fig. 2(a) for neat epoxy and in Fig. 2(b) for GFRP, respectively. The tensile modulus of epoxy at the lowest tested temperature of 25 °C is 3.2 GPa, while that of GFRP is 10.5 GPa. The maximum of the loss factors at 1 Hz were measured for the epoxy at 147.3 °C and for the GFRP at 151 °C. The loss factor of the epoxy was approximately 1.2, while the loss factor of the GFRP was approximately 0.6. At the temperatures, where the parameters were adjusted, no discontinuities or other issues could be seen.

The Wicket plots for both materials are shown in Fig. 3. on the left for epoxy and on the right for GFRP. The isotherms form a continuous line with an arc-like shape, with only minor discontinuities. For the GFRP, a gap between two isotherms above T_g at 160 °C (6 10^2 MPa) can be observed. For epoxy, a discontinuity is visible below T_g at 135 °C (1.5 10^3 MPa), where a little arc is reaching out of the continuous curve.

The application of the TTS to the frequency sweeps is shown in Fig. 4. Hereby, the master curve is created first for the loss factor, which is shown in Fig. 4(a) for epoxy and in Fig. 4(d) for the GFRP. Additionally, the unshifted multiplex is given in the same diagram for each master curve. The master curve for epoxy displays a smooth and continuous shape, devoid of any discontinuities, as also observed for the master curve of GFRP. However, for the GFRP multiplex, two curves corresponding to temperatures of 137.5 °C and 140 °C exhibited no overlap, necessitating the use of interpolation. A comparison of the two master curves reveals that the maximum of the loss factor for GFRP has been shifted to a lower frequency compared to epoxy. For GFRP, the maximum is just above 10^{-10} Hz, while for epoxy it is just below 10^{-7} Hz.

The corresponding shift factors are shown in Figs. 4(b) and 4(e). A discontinuity can be seen for epoxy at 100 °C, where the stress is adjusted the first time. At 150 °C, the shift factor a_T for epoxy is anticipated to be 2.5×10^{-8} and at 2.1×10^{-10} for GFRP. Two distinct gradients can be described for neat epoxy, with a markedly lower gradient observed below 120 °C. The distinction is less apparent in the case of GFRP, where a continuous change in gradient can be described.

The calculated shift factors of the loss factors were then applied to form the master curves of the storage modulus, which are shown in Figs. 4(c) and 4(f). Both master curves exhibit vertical gaps. In the case of the epoxy specimen, small gaps are discernible at temperatures below the glass transition area. For the GFRP specimen, a gap is observable at the end of the glass transition area.

4. Discussion

In order to gain an understanding of the characteristics of a good Wicket plot and those of a poor one, it is recommended that existing curves from the literature be examined. An example of a successful and unsuccessful Wicket plot is provided by Menard [6]. In the case of the unsuccessful Wicket plot, it is evident that arcs of the individual curves extend beyond of the continuous shape. The majority of the Wicket plot of the epoxy, as shown in Fig. 3(a) exhibits a shape that is similar to that of the successful plot. The aforementioned discontinuity, which was described in Section 3, bears resemblance to the extending arcs of the unsuccessful curve. The effect in the master curve can be seen at the E' master curve for epoxy the in Fig. 4(c) as a gap at the concerning temperature.

Guedes showed a Cole-Cole plot and a van-Gurp-Palmen plot for a thermorheologically complex material [20]. Thereby, the curves for the different temperatures clearly do not superimpose because of horizontal gaps between the individual curves, a vertical shifting is therefore necessary. The previously described gap in Fig. 3(b) shows similar behaviour, but concerns only a small temperature range above T_g and is also visible in the E' master curve.

The remaining vertical gaps may be attributed, at least in part, to the influence of temperature and thermal expansion. These effects could be incorporated by the Rouse model [27], as represented by Eq. (2), which is a ratio of temperature and density at two distinct conditions.

$$b_T = \frac{T_0\,\rho_0}{T\,\rho} \tag{2}$$

In general, the shapes of the Wicket plots indicate that both the epoxy matrix and the reinforced specimens appear to be thermorheologically simple, except for minor effects.

In a recent study, Shundo et al. investigated a comparable horizontal shift for a DGEBA-based epoxy with a log a_T value of −10 in a temperature range from T_g to 65 K above T_g [28]. However, the higher shift of GFRP compared to that of neat epoxy is nonetheless an important aspect. On the one hand, Mäder et al. created a master curve for the storage modulus of DGEBA-based epoxy and unidirectional

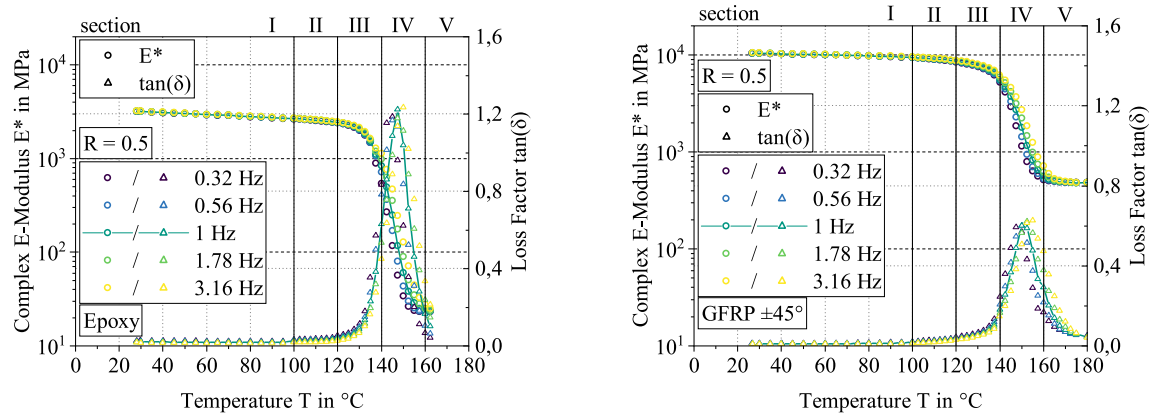

(a) neat epoxy with the maximal stress of 2.9 MPa in section I, 2 MPa in section II, 1.6 MPa in section III, 0.4 MPa in section IV and in section V

(b) $[+45/-45]_{2s}$ fibre-reinforced epoxy with the maximal stress of 10.2 MPa in section I, 8.2 MPa in section II, 6.1 MPa in section III, 1.2 MPa in section IV and 0.5 MPa in section V.

Fig. 2. DMTA temperature sweeps of the complex E-modulus and the loss factor.

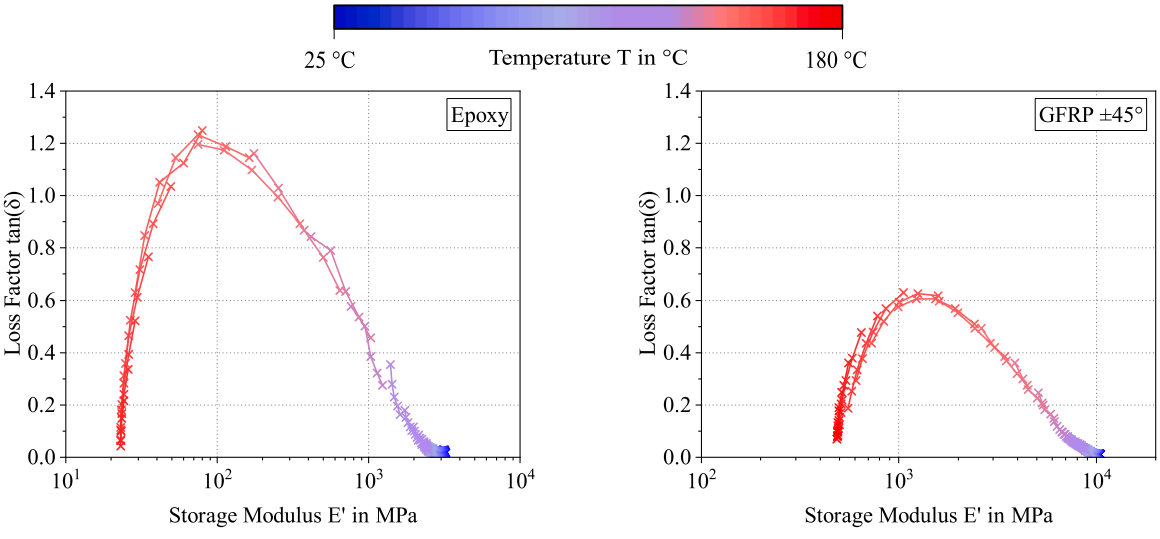

(a) neat epoxy

(b) $[+45/-45]_{2s}$ fibre-reinforced epoxy

Fig. 3. DMTA temperature sweeps of the complex E-modulus and the loss factor.

glass-fibre-reinforced epoxy and determined that the fibres tend to considerably retard the matrix relaxation process [29]. On the other hand, Miyano et al. compared the horizontal shifting of flexural static strength at different deflection rates of a satin-woven carbon-fibre-reinforced epoxy and the neat epoxy. The two shift factors agreed well with each other [30]. They explained the similarity with the failure mechanism, which is controlled by the viscoelastic behaviour of the matrix. Including the continuously increasing gradient, the course is similar to the shift factor determined in this paper. A more defined transition between the two gradients was seen for the horizontal shifting of the storage modulus for a dynamic viscoelastic test of quasi-isotropic carbon-fibre-reinforced epoxy [31]. In the explanation of Miyano et al. the fibres must act in the elastic region as an ideal elastic component with constant stiffness over the temperature, therefore, the differences in shifting must be owing to a different fibre-matrix interaction or an effect of sizing. It should be noted that the neat epoxy is under tensile stress, whereas the epoxy in the GFRP in this work is under shear stress due to the $[+45/-45]_{2s}$ fibre orientation. Laminates with different fibre orientations might behave differently. In a [0] laminate, the epoxy is predominantly under tensile stress and the influence of the epoxy will be lower, taking into account the significantly higher stiffness of the fibres.

Furthermore, the load was adjusted according the stiffness in five sections. It is important to emphasise that the viscoelastic non-linearity and thereby, the TTS of the polymer are influenced by the load. Consequently, the influence of varying load levels cannot be excluded.

One potential explanation for the higher shifting of the GFRP specimen is that the maximum of tan(δ) was determined at a temperature that is 3.7 K higher than that of neat epoxy. This effect causes a difference in shifting $\Delta\log a_T$ of the maximum of tan(δ) of approximately 0.6 to 0.8. A change in T_g may be attributed to the chemical impact of the sizing. The Fox equation (3) may be used to describe a changed T_g resulting from the presence of a second phase, with the weight fractions ω of the components A and B [32].

$$\frac{1}{T_g} = \frac{\omega_A}{T_{gA}} + \frac{\omega_B}{T_{gB}} \tag{3}$$

Mäder et al. measured for a DGEBA-based epoxy, a significantly lower T_g (99–100 °C instead of 106 °C) when it was reinforced with unidirectional glass fibres also without sizing [29].

A greater proportion of the different horizontal shifting occur at temperatures just below the glass-transition area, specifically between 80 °C and 120 °C. Above and below this temperature range, log a_T of both materials have a similar slope. In the region of lower measured temperatures, the values of tan(δ) have a very small slope, especially

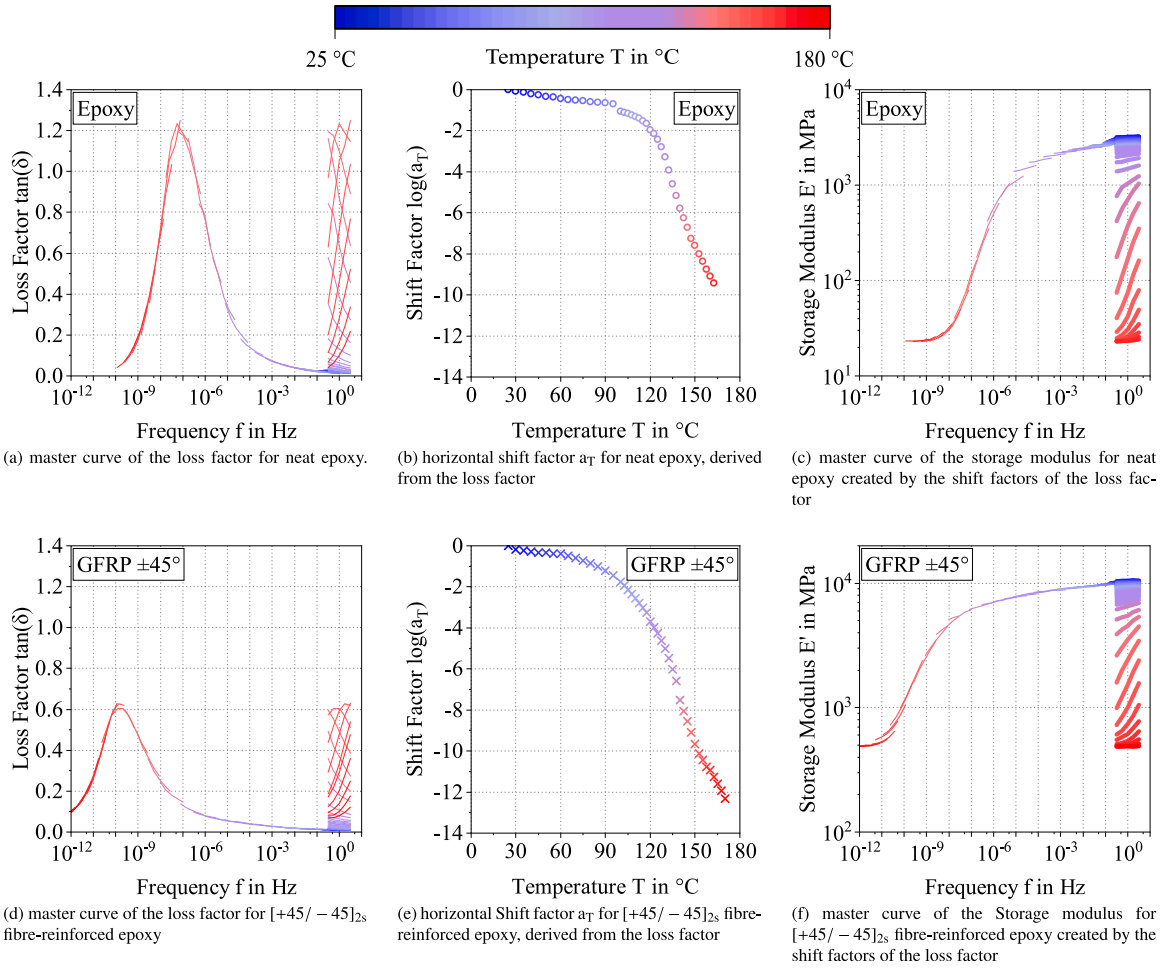

(a) master curve of the loss factor for neat epoxy.

(b) horizontal shift factor a_T for neat epoxy, derived from the loss factor

(c) master curve of the storage modulus for neat epoxy created by the shift factors of the loss factor

(d) master curve of the loss factor for $[+45/-45]_{2s}$ fibre-reinforced epoxy

(e) horizontal Shift factor a_T for $[+45/-45]_{2s}$ fibre-reinforced epoxy, derived from the loss factor

(f) master curve of the Storage modulus for $[+45/-45]_{2s}$ fibre-reinforced epoxy created by the shift factors of the loss factor

Fig. 4. Created master curves for neat epoxy and $[+45/-45]_{2s}$ fibre-reinforced epoxy.

for the neat epoxy, leading to a very small shift, as the individual curves are already close to overlapping. In the case of GFRP, the values of tan(δ) show a slight increase at lower temperatures compared to neat epoxy, resulting in a higher shift. It is possible that this earlier increase is owing to increased stress at the fibre-matrix interfaces, particularly at fibre crossing points and owing to fibre entrapment, resulting in increased energy consumption at lower temperatures.

The stepwise reduction in the magnitude of the mechanical load during DMTA enabled the measurement of whole datasets below and above T_g with a single specimen. As a DMTA is conducted within the lower linear elastic region of the material, any changes resulting from altered load magnitude should be minimal.

5. Conclusion

This study introduces a novel approach to addressing stiffness changes in materials during DMTA. Furthermore, master curves according to TTS were created by a refined method and the neat and fibre-reinforced epoxy shifting were compared. By stepwise adjusting the mechanical load during testing, we successfully overcame the challenge of stiffness reduction, demonstrating that variations in load magnitude have negligible effects on the accuracy of the DMTA measurement. This advancement provides a robust and simple methodology for handling materials with varying stiffness. Master curves were created by shifting the loss factor and applying the generated horizontal shift factors to the storage modulus. The horizontal shift factor of GFRP was found to be higher compared to the neat matrix system. Wicket plots were discussed and used to verify the applicability of TTS. Both the continuous fibre-reinforced epoxy and the matrix material exhibited mostly thermorheologically simple behaviour. In addition, a comparative analysis was performed between the two materials.

CRediT authorship contribution statement

Daniel Esse: Writing – review & editing, Writing – original draft, Visualization, Validation, Software, Resources, Project administration, Methodology, Investigation, Formal analysis, Data curation, Conceptualization. **Benedikt Scheuring:** Writing – review & editing, Conceptualization. **Frank Henning:** Supervision. **Wilfried V. Liebig:** Writing – review & editing, Supervision, Funding acquisition, Conceptualization.

Declaration of competing interest

The authors declare that they have no known competing financial interests or personal relationships that could have appeared to influence the work reported in this paper.

Acknowledgements

This research was funded by the Deutsche Forschungsgemeinschaft (DFG, German Research Foundation), grant number LI 3675/1-1. The authors acknowledge support by the KIT-Publication Fund of the Karlsruhe Institute of Technology.

Data availability

Data will be made available on request.

References

[1] V. Pistor, F.G. Ornaghi, L. Heitor, A.J. Zattera, Dynamic mechanical characterization of epoxy/epoxycyclohexyl–POSS, Mater. Sci. Eng. A 532 (2012) 339–345.

[2] H.L. Ornaghi, V. Pistor, Z. A.J., Effect of the epoxycyclohexyl polyhedral oligomeric silsesquioxane content on the dynamic fragility of an epoxy resin, J. Non-Cryst. Solids 358 (2) (2012) 427–432.

[3] N. Taheri Qazvini, N. Mohammadi, Dynamic mechanical analysis of segmental relaxation in unsaturated polyester resin networks: Effect of styrene content, Polymer 46 (21) (2005) 9088–9096.

[4] W.V. Liebig, A. Jackstadt, V. Sessner, K.A. Weidenmann, L. Kärger, Frequency domain modelling of transversely isotropic viscoelastic fibre-reinforced plastics, Compos. Sci. Technol. 180 (2019) 101–110.

[5] K.S. Cho, Viscoelasticity of Polymers, Springer, 2016.

[6] K. Menard, Dynamic Mechanical Analysis: A Practical Instruction, CRC Press, 2008.

[7] J. Capodagli, R. Lakes, Isothermal viscoelastic properties of PMMA and LDPE over 11 decades of frequency and time: a test of time–temperature superposition, Rheol. Acta 47 (2008) 777–786.

[8] J.D. Ferry, Viscoelastic Properties of Polymers, John Wiley & Sons, 1980.

[9] R. Li, Time-temperature superposition method for glass transition temperature of plastic materials, Mater. Sci. Eng. A 278 (1–2) (2000) 36–45.

[10] Y.S. Urzhumtsev, Time-temperature superposition. Review, Polym. Mech. 11 (1) (1975) 57–72.

[11] D.G. Fesko, N.W. Tschoegl, Time-temperature superposition in thermorheologically complex materials, J. Polym. Sci. C 35 (1971) 51–69.

[12] M. Van Gurp, J. Palmen, Time-temperature superposition for polymeric blends, Rheol. Bull. 67 (1) (1998) 5–8.

[13] D.J. Plazek, I.C. Chay, K.L. Ngai, C.M. Roland, Viscoelastic properties of polymers. 4. Thermorheological complexity of the softening dispersion in polyisobutylene, Macromolecules 28 (19) (1995) 6432–6436.

[14] P.H.P. Macaúbas, N.R. Demarquette, Time-temperature superposition principle applicability for blends formed of immiscible polymers, Polym. Eng. Sci. 42 (7) (2002) 1509–1519.

[15] J. Honerkamp, J. Weese, A note on estimating mastercurves, Rheol. Acta 32 (1993) 57–64.

[16] M.A. Kraus, M. Niederwald, Generalized collocation method using stiffness matrices in the context of the theory of linear viscoelasticity (GUSTL), Tech. Mech. Eur. J. Eng. Mech. 37 (1) (2017) 82–106.

[17] M. Gergesova, I. Saprunov, I. Emri, Closed-form solution for horizontal and vertical shiftings of viscoelastic material functions in frequency domain, Rheol. Acta 55 (2016) 351–364.

[18] S. Naya, A. Meneses, J. Tarrío-Saavedra, R. Artiaga, J. López-Beceiro, C. Gracia-Fernández, New method for estimating shift factors in time–temperature superposition models, J. Therm. Anal. Calorim. 113 (2013) 453–460.

[19] K. Cho, Geometric interpretation of time-temperature superposition, Korea Aust. Rheol. J. 21 (1) (2009) 13–16.

[20] R.M. Guedes, A viscoelastic model for a biomedical ultra-high molecular weight polyethylene using the time–temperature superposition principle, Polym. Test. 30 (3) (2011) 294–302.

[21] D. George, E.A. Peraza Hernandez, R.C. Lo, M. Madou, Fabrication of polymer and carbon polyhedra through controlled cross-linking and capillary deformations, Soft Matter 15 (45) (2019) 9171–9177.

[22] J. Schalnat, D.G. Gómez, L. Daelemans, I. De Baere, K. De Clerck, W. Van Paepegem, Influencing parameters on measurement accuracy in dynamic mechanical analysis of thermoplastic polymers and their composites, Polym. Test. 91 (2020) 106799.

[23] Q. Shao, P. Lee-Sullivan, Guidelines for performing storage modulus measurements using the ta instruments DMA 2980 three-point bend mode II. Contact stresses and machine compliance, Polym. Test. 19 (3) (2000) 239–250.

[24] P. Lee-Sullivan, D. Dykeman, Guidelines for performing storage modulus measurements using the TA Instruments DMA 2980 three-point bend mode: I. Amplitude effects, Polym. Test. 19 (2) (2000) 155–164.

[25] I.M. McAninch, G.R. Palmese, J.L. Lenhart, J.J. La Scala, DMA testing of epoxy resins: The importance of dimensions, Polym. Eng. Sci. 55 (12) (2015) 2761–2774.

[26] H.F. Brinson, L.C. Brinson, et al., Polymer engineering science and viscoelasticity, An Introd. 99 (2008) 157.

[27] P.E. Rouse, A theory of the linear viscoelastic properties of dilute solutions of coiling polymers, J. Chem. Phys. 21 (7) (1953) 1272.

[28] A. Shundo, M. Aoki, S. Yamamoto, K. Tanaka, Effect of cross-linking density on horizontal and vertical shift factors in linear viscoelastic functions of epoxy resins, Macromolecules 54 (20) (2021) 9618–9624.

[29] E. Mäder, S. Gao, R. Plonka, Static and dynamic properties of single and multi-fiber/epoxy composites modified by sizings, Compos. Sci. Technol. 67 (6) (2007) 1105–1115.

[30] Y. Miyano, M. Nakada, M.K. McMurray, R. Muki, Prediction of flexural fatigue strength of CRFP composites under arbitrary frequency, stress ratio and temperature, J. Compos. Mater. 31 (6) (1997) 619–638.

[31] Y. Miyano, M. Nakada, K. Nishigaki, Prediction of long-term fatigue life of quasi-isotropic CFRP laminates for aircraft use, Int. J. Fatigue 28 (10) (2006) 1217–1225.

[32] R.E. Jensen, E. O'Brien, J. Wang, J. Bryant, T.C. Ward, L.T. James, D.A. Lewis, Characterization of epoxy–surfactant interactions, J. Polym. Sci. Part B: Polym. Phys. 36 (15) (1998) 2781–2792.